

Soliton Mobility in Disordered Lattice

Zhi-Yuan Sun* and Shmuel Fishman

Department of Physics, Technion-Israel Institute of Technology, Haifa 32000, Israel

Avy Soffer

Department of Mathematics, Rutgers University, New Jersey 08854, U.S.A

(Dated: July 4, 2018)

We investigate soliton mobility in the disordered Ablowitz-Ladik (AL) model and the standard nonlinear Schrödinger (NLS) lattice with the help of an effective potential generalizing the Peierls-Nabarro potential. This potential results from deviation from integrability, resulting of randomness for the AL model, and of both randomness and lattice discreteness for the NLS lattice. Statistical properties of such a potential are analyzed, and it is shown how the soliton mobility is affected by its size. The usefulness of this effective potential in studying soliton dynamics is demonstrated numerically. Further we propose two ways the soliton transport in presence of disorder can be enhanced: one is to use specific realizations of randomness, and the other one is to consider a specific soliton pair.

PACS numbers: 05.45.Yv, 42.65.Tg

Introduction—Discrete solitons (including breathers—in our discussion referred as the localized modes of soliton type but with temporarily oscillating profiles) for the nonlinear Schrödinger (NLS) type models on a lattice, have been theoretically and experimentally studied in various areas of physics, e.g., in nonlinear optics and solid-state physics [1–4]. These localized modes can exist in the interplay of the nonlinearity and discreteness, and their mobility is one of the most important aspects, for considering the mass and energy transport in a lattice. One effective path to physically understand mobility of the discrete soliton is using the description in terms of the Peierls-Nabarro (PN) potentials [5, 6]. It could be understood as a type of effective potential, resulting of deviation from integrability (we will obtain similar deviation results of randomness for the disordered AL model, and of both randomness and discreteness for the disordered NLS lattice), with its amplitude being viewed as a minimum barrier that the soliton should overcome to propagate in the lattice. By virtue of such a concept, a series of works investigated mobility of discrete solitons in various NLS lattices [6–8].

One practical method to calculate the effective potential is employing a collective coordinate approximation [5, 6], with the assumption that the discrete soliton propagates very slowly and adiabatically. In this potential the soliton can be considered as an effective particle. Such adiabatic approach provides a good approximate picture when the radiation is negligible.

In the present paper, we will study solitons for the AL model and the standard NLS lattice in presence of disorder using similar methods. Our investigations are relevant for experiments using random media in optics [9] and optical speckle potentials in Bose-Einstein conden-

sates [10]. On the other hand, nonlinearity and disorder are found to play important roles in existence and stability of the localized excitation in a trimer model [11]. We will analyze statistical properties of the generalized PN effective potential, and show how these affect the soliton mobility. We will mainly focus on the relatively short-time-scale soliton behavior, with the lattice soliton initially injected with a small amount of kinetic energy (moving slowly), and emitting negligible radiation. Under such situations, certain basic features related to the PN effective potential are believed to be revealed.

Soliton mobility in Ablowitz-Ladik lattice with disorder—We start from the integrable Ablowitz-Ladik (AL) model [12], with a random potential term, defined by

$$i\dot{\psi}_n = -(\psi_{n-1} + \psi_{n+1})(1 + |\psi_n|^2) + \varepsilon_n \psi_n, \quad (1)$$

where ψ_n is the wavefunction at site n and time t , while ε_n is the normally distributed random potential (uncorrelated) with zero mean value and standard variance σ , that is, $\langle \varepsilon_n \rangle = 0$ and $\langle \varepsilon_n \varepsilon_{n'} \rangle = \sigma^2 \delta(n - n')$. Integrability of the AL model in absence of the potential leads its PN potential barrier to vanish [5] (as well as vanishing of the resonances that generate radiation [2]), and admits an exact mobile soliton solution at arbitrary velocity, written as

$$\psi_n(t) = \frac{\sinh(\mu)}{\cosh[\mu(n-x)]} \exp[ik(n-x) + i\alpha], \quad (2)$$

where (without disorder) the time-dependent parameters x and α can be expressed as $\dot{x} = 2 \frac{\sinh(\mu)}{\mu} \sin(k)$ and $\dot{\alpha} = 2[\cosh(\mu) \cos(k) + \frac{k}{\mu} \sinh(\mu) \sin(k)]$. We now assume the random potential is weak and the soliton velocity is slow, then apply the adiabatic approximation [13, 14] to derive the evolution equations for the soliton parameters x and

* sunzhiyuan137@aliyun.com

k with disorder (assuming $\dot{\mu} = 0$)

$$\dot{x} = \frac{2 \sinh(\mu)}{\mu} \sin(k), \quad (3a)$$

$$\dot{k} = - \sum_{n=-\infty}^{+\infty} \frac{\varepsilon_n \sinh^2(\mu) \tanh[\mu(n-x)]}{\cosh[\mu(n+1-x)] \cosh[\mu(n-1-x)]}. \quad (3b)$$

For the system (3), the effective potential, regarded as the PN potential, can be written as

$$U(x) = - \int_0^x f(\xi) d\xi, \quad (4)$$

with the equivalent force $f(\xi) = \sum \varepsilon_n \phi(n - \xi)$, where

$\phi(z) = -\frac{\sinh^2(\mu) \tanh(\mu z)}{\cosh[\mu(z+1)] \cosh[\mu(z-1)]}$. The force $f(\xi)$ also has zero mean value, and its correlation function r_f can be derived due to its linear property,

$$r_f(\xi, \xi') = \langle f(\xi) f(\xi') \rangle = \sigma^2 \sum_{n=-\infty}^{+\infty} \phi(n-\xi) \phi(n-\xi'). \quad (5)$$

Using the Poisson summation formula and residue theorem, we can evaluate the sums in (5), and obtain

$$r_f(\xi, \xi') = \sigma^2 \left[\mathfrak{R}_0(\mu, \Delta\xi) + 2 \sum_{s=1}^{+\infty} \mathfrak{R}_s(\mu, \xi, \Delta\xi) \right], \quad (6)$$

where $(\Delta\xi = \xi - \xi')$,

$$\mathfrak{R}_0 = \sinh^2(\mu) \{ 2\Delta\xi \coth(\mu\Delta\xi) \operatorname{csch}[\mu(\Delta\xi - 1)] \operatorname{csch}[\mu(\Delta\xi + 1)] - (\Delta\xi - 2) \coth[\mu(\Delta\xi - 1)] \operatorname{csch}[\mu(\Delta\xi - 2)] \operatorname{csch}(\mu\Delta\xi) - (\Delta\xi + 2) \coth[\mu(\Delta\xi + 1)] \operatorname{csch}[\mu(\Delta\xi + 2)] \operatorname{csch}(\mu\Delta\xi) \}, \quad (7a)$$

$$\begin{aligned} \mathfrak{R}_s = & \frac{\pi \sinh^2(\mu)}{\mu} \operatorname{csch}\left(\frac{\pi^2 s}{\mu}\right) \cos[\pi s(2\xi - \Delta\xi)] \{ 2 \coth(\mu\Delta\xi) \operatorname{csch}[\mu(\Delta\xi + 1)] \operatorname{csch}[\mu(\Delta\xi - 1)] \sin(\pi s \Delta\xi) \\ & - \coth[\mu(\Delta\xi - 1)] \operatorname{csch}(\mu\Delta\xi) \operatorname{csch}[\mu(\Delta\xi - 2)] \sin[\pi s(\Delta\xi - 2)] \\ & - \coth[\mu(\Delta\xi + 1)] \operatorname{csch}(\mu\Delta\xi) \operatorname{csch}[\mu(\Delta\xi + 2)] \sin[\pi s(\Delta\xi + 2)] \}. \end{aligned} \quad (7b)$$

Eqs. (6) and (7) apparently show that, due to discreteness, $f(\xi)$ is a nonstationary random process (depending

not only on $\Delta\xi$) [15]. With (6), we derive the variance of $f(\xi)$ as

$$\sigma_f^2(\xi)/\sigma^2 = r_f(\xi' \rightarrow \xi)/\sigma^2 = 3 \coth(\mu) - \tanh(\mu) - \frac{3}{\mu} - \frac{6\pi^2}{\mu^2} \sum_{s=1}^{+\infty} s \operatorname{csch}\left(\frac{\pi^2 s}{\mu}\right) \cos(2\pi s \xi). \quad (8)$$

Generally speaking, when $\mu \ll 1$, $f(\xi)$ can be approximately seen as a stationary random process, with $\sigma_f^2/\sigma^2 \approx 3 \coth(\mu) - \tanh(\mu) - \frac{3}{\mu}$ (when $\mu \lesssim 0.3$, it accords well with the continuous limit result $\sigma_f^2/\sigma^2 = \frac{4 \sinh^4(\mu)}{15\mu} \approx \frac{4}{15}\mu^3$); when $1 \lesssim \mu \lesssim 3$, $f(\xi)$ is a nonstationary random process with a periodic variance (the terms for $s \geq 2$ are neglected as small terms) $\sigma_f^2(\xi)/\sigma^2 \approx 3 \coth(\mu) - \tanh(\mu) - \frac{3}{\mu} - \frac{6\pi^2}{\mu^2} \operatorname{csch}\left(\frac{\pi^2}{\mu}\right) \cos(2\pi\xi)$; when $\mu \gtrsim 3$, we may have to consider overlap of the terms with $s \geq 2$. We numerically calculate the force $f(\xi)$ for a large number of realizations of the random potential to derive its variance, and make a comparison with (8). Good agreement can be seen in Fig. 1(a), for two different regimes.

With the statistical property of the force $f(\xi)$, we next consider the effective potential $U(x)$. Apparently, it is a nonstationary random process with zero mean value, and

its correlation function can be derived as

$$r_U(x, x') = \langle U(x) U(x') \rangle = \int_0^x \int_0^{x'} r_f(\xi, \xi') d\xi d\xi'. \quad (9)$$

We can numerically integrate (9) with appropriate truncation of (6) according to the value of μ , and further obtain the variance of $U(x)$ as

$$\sigma_U^2(x)/\sigma^2 = r_U(x' \rightarrow x)/\sigma^2. \quad (10)$$

Three typical examples of (10), compared to numerical results found sampling various realizations using (4), are shown in Fig. 1(b). We can see that, after an increase in short distance, σ_U/σ approaches a periodic type function (for small enough μ , the periodicity can be neglected, e.g., $\mu = 0.5$) with a nonzero mean value (averaged in finite periods along x). We denote such mean value as

$\sigma_U^{(m)}/\sigma$, where $\sigma_U^{(m)}$ is theoretically defined as

$$\sigma_U^{(m)} = \lim_{L \rightarrow \infty} \frac{1}{L} \int_0^L \sigma_U(x) dx, \quad (11)$$

and further compute that the amplitude of the periodic function is not more than 6% of $\sigma_U^{(m)}/\sigma$, even up to $\mu = 6$. Thus, $\sigma_U^{(m)}$ can be employed, in the sense of statistics, as the PN-type potential barrier that relates the soliton mobility in presence of disorder. $\sigma_U^{(m)}/\sigma$ as a function of μ , is presented in Fig. 1(c), as well as the comparison with numerical results for multiple realizations of the random potentials. Generally speaking, the smaller soliton has a larger mobility due to its smaller effective potential barrier, however, there exist approximately two regimes: one is the *sharp slope* regime ($\mu \lesssim 1$) where $\sigma_U^{(m)}/\sigma$ decreases quickly with μ decreasing; the other one is the *flat slope* regime ($\mu \gtrsim 3$) where $\sigma_U^{(m)}/\sigma$ decreases considerably slowly with μ decreasing.

To check such mobility, we directly proposed numerical simulation of Eq. (1), with the soliton solution (2) as the initial condition. The soliton behavior was observed for more than 100 realizations of random potentials with

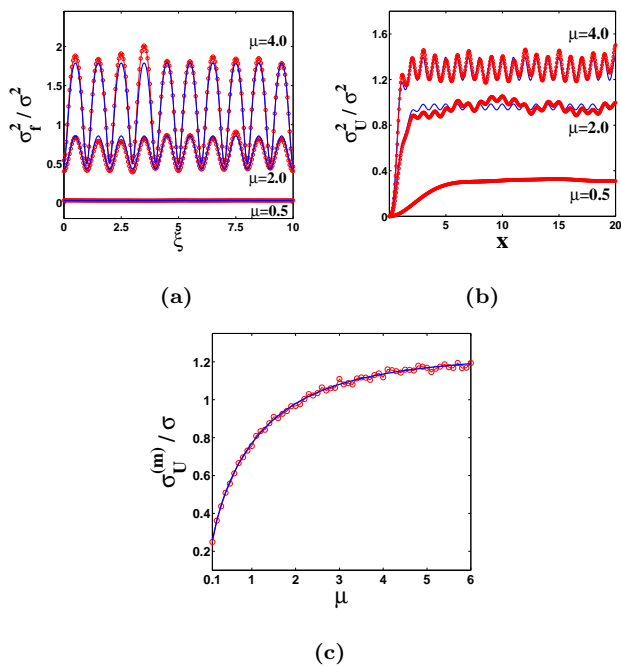


FIG. 1. (Color online) Statistical properties of the equivalent force $f(\xi)$ and effective potential $U(x)$. The blue solid lines represent the results from (8) or (10), and the red circles represent the statistically simulated results. In simulation, we discretize the coordinate with $\Delta\xi = 0.05$, and the variance is computed for 10^3 realizations of random potentials. (a) Comparison between the statistically simulated variance σ_f^2/σ^2 and (8) for $\mu = 0.5, 2.0$, and 4.0 ($\sigma = 0.02$). (b) Comparison between the statistically simulated variance σ_U^2/σ^2 and (10). (c) $\sigma_U^{(m)}/\sigma$ of (11) as a function of μ .

$\sigma = 0.01$, and the soliton was given a small initial velocity $v_0 = 0.3$ for each realization. Two typical results, with the soliton center of mass x_c as function of t , are presented in Figs. 2(a) and (b). We can see that, no matter whether the soliton decelerates or accelerates (on average) for some time, the larger soliton is reflected or trapped by the randomness stronger than the small soliton. In principle, the soliton reflects near some large effective potential barrier, or gets trapped between two large barriers. Before the first reflection, whether deceleration or acceleration occurs, is depending on the details of the random potential. Generally, we can approximately use a time difference to identify such deceleration (acceleration) stage, defined as

$$\tau(x) = \int_0^x dx \left[\frac{\mu}{2 \sinh(\mu) \sin(k)} - \frac{1}{v_0} \right], \quad (12)$$

where $\cos(k) = \frac{\mu}{2 \sinh(\mu)} U(x) + \cos(k_0)$, as derived from the conservation of the effective total energy $H = -\frac{2 \sinh(\mu)}{\mu} \cos(k) + U(x)$. Thus, if $\tau < 0$, there exists an averaged acceleration process within $[0, x]$ (before first reflection); while $\tau > 0$, it is an averaged deceleration process. One interesting idea is to use the region where randomness accelerates the soliton in finite time. For instance, as seen in Fig. 2(b), for relatively large soliton, we may choose the random potential sections before the first reflection point, and arrange them periodically, to realize the mass transport in one direction for some time.

Another aspect is to consider a pair of solitons, where one is large and the other one is small, with the same initial velocity and a short separation distance between them (may be partially overlapped). In order to enhance transportation of the large soliton, we arrange the small one to follow the large one, and give them an initial phase difference π that provides a repulsive interaction between both solitons. When the large soliton encounters a large effective potential barrier that would obstruct its mobility, while the small one might be still well propagating due to its larger mobility, and is expected to *push* the large one to *help* it overcome the barrier. A similar mechanism to trigger a migration by a low-amplitude

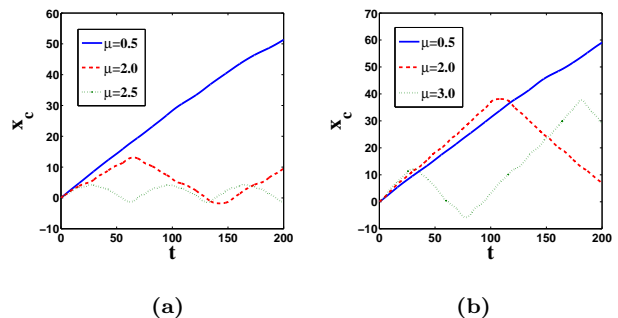


FIG. 2. (Color online) Soliton center of mass x_c as a function of time t for two typical realizations of random potentials ($\sigma = 0.01$ and $v_0 = 0.3$), found from (1).

solitary wave that collides with an excitation has been described for a pure NLS lattice [16]. As an example, such idea is realized and illustrated in Fig. 3 for a specific realization of randomness. Fig. 3(a) presents a large single soliton ($\mu = 2$) trapped by the random potential, while in Fig. 3(b), we add the auxiliary small soliton ($\mu = 0.5$) with the separation distance of 5. It shows that the large soliton can now propagate without reflection or trapping for some time. The interaction of the small soliton ($\mu = 0.5$), with the large one results in the motion of the large soliton in the same direction without reflection. Similar results were found also for other realizations of the disorder.

For the large soliton, the randomness-induced radiation is still very small for considerably long time, and the soliton behavior can be well described by the effective potential [a typical comparison is shown in Fig. 4(a) up to $t = 10^4$]. Generally speaking, the large soliton is apt to be trapped by the randomness after some sequences of deceleration and acceleration periods (the soliton behavior was observed in the long-time simulation for more than 10 realizations of the random potential). For the small soliton, if the randomness is weak enough, the effective potential also gives a good approximation for long time. In Fig. 4(b), we decrease the strength of the random potential from the left to the right panels, and show that the effective potential approach agrees better with the numerical solutions of Eq. (1) for weaker randomness. On the other hand, if the randomness is relatively strong, the small soliton was observed to continue radiating its mass and kinetic energy during the long-time propagation, and even exhibit visible deformation on its profile. Such a case may be analyzed using the method of modulation equation [17], which is not within the scope of this paper.

Behavior for the standard NLS lattice with disorder—We study the standard NLS lattice

$$i\dot{\psi}_n = -(\psi_{n-1} + \psi_{n+1}) - \nu|\psi_n|^2\psi_n + \varepsilon_n\psi_n. \quad (13)$$

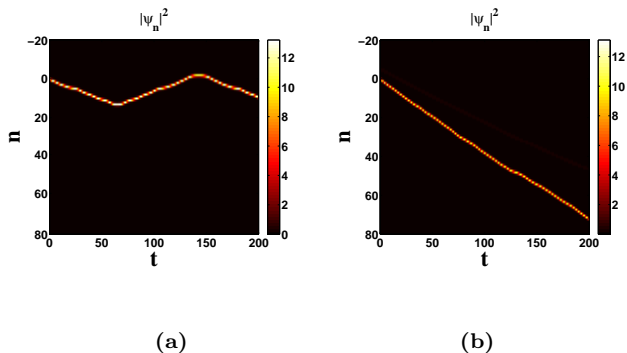


FIG. 3. (Color online) Intensity map of the soliton propagation in a realization of random potential with $\sigma = 0.01$. (a) A single soliton with $\mu = 2$ and $v_0 = 0.3$. (b) A pair of solitons with $\mu_1 = 2$, $\mu_2 = 0.5$, and $v_0 = 0.3$. The initial separation distance Δx and phase difference $\Delta\alpha$ are 5 and π , respectively.

We consider this equation as the AL model with a perturbation term on the RHS, $R_n = |\psi_n|^2(\psi_{n+1} + \psi_{n-1} - \nu\psi_n) + \varepsilon_n\psi_n$, and use the adiabatic approximation to derive the similar generalized PN effective potential when μ is not too large ($\mu \ll 3$),

$$\mathcal{U}(x) = -\frac{2\pi^2\nu\sinh^2(\mu)}{\mu^3\sinh\left(\frac{\pi^2}{\mu}\right)}\cos(2\pi x) + U(x), \quad (14)$$

where $\dot{x} = 0$ and $\dot{x} \approx 2\sinh(\mu)\tanh(\mu)\sin(k)/\mu^2$, and $U(x)$ is the same randomness generated effective potential (4). In the limit $\mu \rightarrow 0$, the soliton is wide, therefore the discreteness of the lattice is not important, and the result of the continuous integrable model is approached. Naturally, we may use the following parameter to approximately decide which factor dominates,

$$\kappa = \sigma_U^{(m)} / \frac{2\pi^2\nu\sinh^2(\mu)}{\mu^3\sinh\left(\frac{\pi^2}{\mu}\right)} = \frac{\sigma}{\nu} \left[\frac{\mu^3\sinh\left(\frac{\pi^2}{\mu}\right)\lambda(\mu)}{2\pi^2\sinh^2(\mu)} \right], \quad (15)$$

where $\lambda(\mu)$ denotes the curve presented in Fig. 1(c). For the typical parameters $\sigma = 0.01$ and $\nu = 1$, when $\mu \ll 1$, $\kappa \gg 1$, the randomness dominates the soliton behavior; when $\mu \approx 1$, $\kappa \approx 2.6$, these two potentials are of the same magnitude; when $\mu \gg 1$, $\kappa \ll 1$, the influence of randomness can be ignored. And, if the soliton is not too large, influence of the randomness on the soliton mobility, with regard to its size, is similar to that found for the model (1).

Here we make some comments: in fact, if the soliton is very small, it is easy to emit relatively strong radiation induced by the randomness, even to be greatly destroyed on its profile. Such a condition may be remarkably out of the adiabatic approximation. If the soliton is very large, its mobility becomes much smaller, due to the large potential barrier of discreteness. On the other hand, strictly speaking, the *soliton* discussed here should

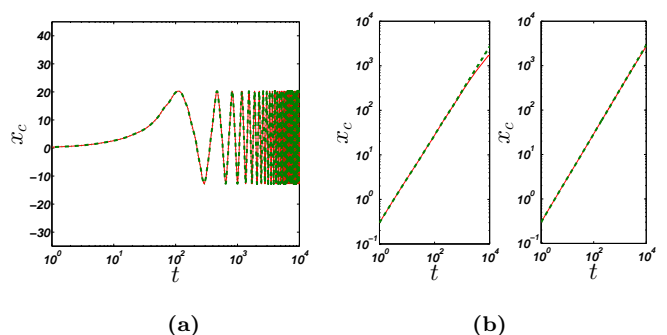


FIG. 4. (Color online) Comparison of the soliton trajectory x_c obtained by numerically integrating Eq. (1) (red solid line) and effective potential approach using $U(x)$ of (4) (green dashed line). (a) The random potential ε used is of $\sigma = 0.01$, and the soliton parameters are $\mu = 1.0$ and $v_0 = 0.3$. (b) Left Panel: the random potential is $\varepsilon' = 0.5\varepsilon$; Right Panel: $\varepsilon' = 0.2\varepsilon$. The soliton parameters are $\mu = 0.5$ and $v_0 = 0.3$.

be replaced by the *breather* ($\dot{\mu} \neq 0$), however, for some parameters, our study may generally and effectively provides a physical description of the lattice soliton mobility with disorder. As an example, we give a set of simulation results in Fig. 5. We know that, Eq. (13) with $\varepsilon_n = 0$ has no exact mobile soliton (breather) solutions, however, we could start from a sech type soliton, after initially emitting a small part of radiation, to numerically generate an approximate breather solution that can propagate for considerably long time [18]. In Fig. 5(a), we generate such two breathers, one is small (the upper panel), the other one is large (the lower panel), with almost the same small velocity. Then, we add a realization of the random potential, and show the simulation result in Fig. 5(b). Apparently, we can see that, the mobility of the large breather is obstructed by the randomness, while the small one is nearly not affected, which is the similar feature as shown in Fig. 2.

Conclusions—With help of the generalized PN effective potential, we investigated mobility of lattice solitons in presence of disorder. We analyzed methods to enhance the mobility of solitons of the AL model (1) in a weak random potential. In some situations (weak randomness and short time), these can be considered as particles moving in the effective potential $U(x)$ of (4). We find two ways to enhance mobility: (a) introducing a random potential that is engineered so that intervals of the random potential where acceleration takes place appear one after the other; (b) a small soliton is arranged to push a large one. The effective potential acting on the soliton results of the deviation from integrability. For the AL model (1) that is integrable in absence of randomness, the potential results of the randomness. For the *standard* NLS lattice (13), the deviation from integrability results of both randomness and discreteness,

as it is integrable in the continuum limit in absence of randomness. The effect of the deviations results in the

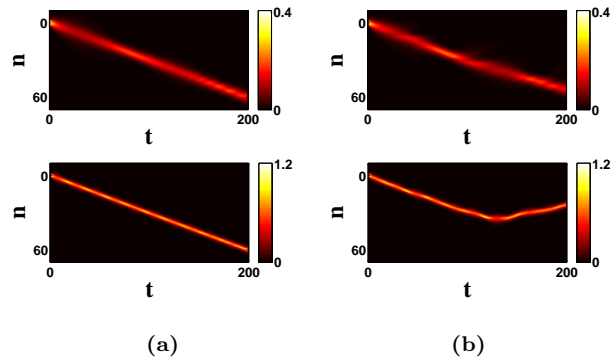


FIG. 5. (Color online) (a) Intensity $|\psi_n|^2$ for two generated breathers of the NLS lattice (13) ($\varepsilon_n = 0$) with almost the same velocity $v \approx 0.30$. The initial conditions are chosen as (2) with $\mu = 0.60$ and $k = 0.150$ for the upper panel, while $\mu = 0.95$ and $k = 0.178$ for the lower panel ($\nu = 0.9$). (b) The two breathers are propagating in presence of the random potential with $\sigma = 0.018$.

potential (14) that plays the role of $U(x)$ of (4) found for the AL model (1). Therefore similar dynamics of solitons is expected in the regime where the effective potential description is valid.

Z.-Y. S. acknowledges the support in part at the Technion by a fellowship of the Israel Council for Higher Education. This work was partly supported by the Israel Science Foundation (ISF-1028), by the US-Israel Binational Science Foundation (BSF-2010132), by the USA National Science Foundation (NSF DMS 1201394) and by the Shlomo Kaplansky academic chair.

-
- [1] F. Lederer, G. I. Stegeman, D. N. Christodoulides, G. Assanto, M. Segev, and Y. Silberberg, *Phys. Rep.* **463**, 1 (2008).
- [2] S. Flach and A. V. Gorbach, *Phys. Rep.* **467**, 1 (2008).
- [3] S. Aubry, *Physica D* **216**, 1 (2006).
- [4] P. G. Kevrekidis, *The Discrete Nonlinear Schrödinger Equation*, Springer-Verlag (Berlin Heidelberg) (2009).
- [5] Y. S. Kivshar and D. K. Campbell, *Phys. Rev. E* **48**, 3077 (1993).
- [6] M. Johansson and P. Jason, arXiv:1412.0994 (2014).
- [7] L. Hadzievski, A. Maluckov, M. Stepić, and D. Kip, *Phys. Rev. Lett.* **93**, 033901 (2004).
- [8] U. Naether, R. A. Vicencio, and M. Stepić, *Opt. Lett.* **36**, 1467 (2011).
- [9] T. Schwartz, G. Bartal, S. Fishman, and M. Segev, *Nature (London)* **446**, 52 (2007); Y. Lahini, A. Avidan, F. Pozzi, M. Sorel, R. Morandotti, D. N. Christodoulides, and Y. Silberberg, *Phys. Rev. Lett.* **100**, 013906 (2008).
- [10] J. E. Lye, L. Fallani, M. Modugno, D. S. Wiersma, C. Fort, and M. Inguscio, *Phys. Rev. Lett.* **95**, 070401 (2005); D. Clément, A. F. Varón, M. Hugbart, J. A. Retter, P. Bouyer, L. Sanchez-Palencia, D. M. Gangardt, G. V. Shlyapnikov, and A. Aspect, *Phys. Rev. Lett.* **95**, 170409 (2005); C. Fort, L. Fallani, V. Guarrera, J. E. Lye, M. Modugno, D. S. Wiersma, and M. Inguscio, *Phys. Rev. Lett.* **95**, 170410 (2005).
- [11] X.-D. Bai and J.-K. Xue, *Phys. Rev. E* **86**, 066605 (2012).
- [12] M. J. Ablowitz and J. F. Ladik, *J. Math. Phys.* **16**, 598 (1975); **17**, 1011 (1976).
- [13] A. A. Vakhnenko and Yu. B. Gaididei, *Tero. Mat. Fiz.* **68**, 350 (1986) [*Theor. Math. Phys.* **68**, 873 (1987)].
- [14] D. Cai, A. R. Bishop, and N. Grønbech-Jensen, *Phys. Rev. E* **53**, 4131 (1996).
- [15] A. Papoulis and S. U. Pillai, *Probability, Random Variables and Stochastic Processes*, 4th edition, McGraw-Hill Europe (2002).
- [16] B. Rumpf, *Phys. Rev. E* **70**, 016609 (2004).
- [17] A. Soffer, *Proc. Int. Congress of Mathematicians (Madrid, Spain, 2006)*, 459 (2006); A. Soffer and X. Zhao, *J. Phys. A* **48**, 135201 (2015).
- [18] R. Franzosi, R. Livi, G.L. Oppo, and A. Politi, *Nonlinearity* **24**, R89 (2011).